



1 **Distributive rainfall/runoff modelling to determine runoff to baseflow**
2 **proportioning and its impact on the determination of the ecological reserve**

3

4 Andrew Watson¹, Jodie Miller¹, Manfred Fink², Sven Kralisch², Melanie Fleischer², and
5 Willem de Clercq³

6 *1. Department of Earth Sciences, Stellenbosch University, Private Bag XI, Matieland 7602,*
7 *South Africa*

8 *2. Department of Geoinformatics, Friedrich-Schiller-University Jena, Loebdergraben 32,*
9 *07743 Jena, Germany*

10 *3. Stellenbosch Water Institute, Stellenbosch University, Private Bag XI, Matieland, 7602,*
11 *South Africa*

12

13 **Keywords:** rainfall/runoff modelling, Verlorenvlei, J2000, ecological reserve

14 **Abstract**

15 River systems that support high biodiversity profiles are conservation priorities world-wide.
16 Understanding river eco-system thresholds to low flow conditions is important for the
17 conservation of these systems. While climatic variations are likely to impact the streamflow
18 variability of many river courses into the future, understanding specific river flow dynamics
19 with regard to streamflow variability and aquifer baseflow contributions are central to the
20 implementation of protection strategies. While streamflow is a measurable quantity, baseflow
21 has to be estimated or calculated through the incorporation of hydrogeological variables. In
22 this study, the groundwater components within the J2000 rainfall/runoff model were distributed
23 to provide daily baseflow and streamflow estimates needed for ecological reserve
24 determination. The modelling approach was applied to the RAMSAR-listed Verlorenvlei



25 estuarine lake system on the west coast of South Africa which is under threat due to agricultural
26 expansion and climatic fluctuations. The sub-catchment consists of four main tributaries, the
27 Krom Antonies, Hol, Bergvallei and Kruismans. Of these, the Krom Antonies tributary was
28 initially presumed the largest baseflow contributor, but was shown to have significant
29 streamflow variability, attributed to the highly conductive nature of the Table Mountain Group
30 sandstones and quaternary sediments. The Bergvallei tributary was instead identified as the
31 major contributor of baseflow. The Hol tributary was the least susceptible to streamflow
32 fluctuations due to the higher baseflow proportion (56%), as well as the dominance of less
33 conductive Malmesbury shales which underlie this tributary. The estimated flow exceedance
34 probabilities indicated that during the wet cycle (2007-2017) the average inflow supported the
35 evaporative demands if the lake was at 40 % capacity, while during the dry cycle (1997-2008),
36 only 15 % of the lake's capacity would be met. The exceedance probabilities estimated in this
37 study suggest that inflows from the four main tributaries are not enough to support the lake
38 during dry cycles, with the evaporation demand of the entire lake being met only 38 % of the
39 time. This study highlighted the importance of low occurrence events for filling up the lake,
40 allowing for regeneration of lake supported ecosystems. While the increased length of dry
41 cycles are likely to result in the lake drying up more frequently, it is important to ensure that
42 water resources are not overallocated during wet cycles, hindering ecosystem regeneration and
43 prolonging the length of these dry cycle conditions.



44 **1. Introduction**

45 Functioning river systems offer numerous economic and social benefits to society including
46 water supply, nutrient cycling and disturbance regulation amongst others (e.g Costanza et al.,
47 1997; Postel and Carpenter, 1997). As a result, many countries worldwide have endeavoured
48 to protect river ecosystems after provision has been made for basic human needs (eg Rowlston
49 and Palmer, 2002). However, the implementation of river protection has been problematic
50 (Richter, 2010), because many river courses and flow regimes have been severely altered due
51 to socio-economic development. Previously, river health problems were thought to be only a
52 result of low-flow conditions and therefore, if minimum flows were kept above a critical level,
53 the river's ecosystem would be protected (Poff et al., 1997). It is now recognised that a more
54 natural flow regime, which includes floods as well as low and medium flow conditions is
55 required for sufficient ecosystem functioning (Postel and Richter, 2012). For these reasons,
56 before protection strategies can be developed or implemented for a river system, a
57 comprehensive understanding of the river flow regime dynamics is necessary.

58 River flow regime dynamics include consideration of not just the surface water in the river but
59 also other water contributions including runoff, interflow and baseflow which are all essential
60 for the maintenance of the discharge requirements. Taken together these factors all contribute
61 to the determination of what is called the ecological reserve, the minimum environmental
62 conditions needed to maintain the ecological health of a river system (Hughes, 2001). A variety
63 of different methods have been developed to incorporate various river health factors into
64 ecological reserve determination (Acreman and Dunbar, 2004). One of the simplest and most
65 widely applied, is where compensation flows are set below reservoirs and weirs, using flow
66 duration curves to derive mean flow or flow exceedance probabilities (e.g. Souchon and Keith,
67 2001). This approach focusses purely on hydrological indices, which are rarely ecologically
68 valid (e.g. Barker and Kirmond, 1998).



69 More comprehensive methods such as functional analysis are focused on the whole ecosystem,
70 including both hydraulic and ecological data (e.g. Building Block Methodology: King and
71 Louw, 1998). While these methods consider that a variety of low, medium and high flow events
72 are important for maintaining ecosystem diversity, they require specific data regarding the
73 hydrology and ecology of a river system, which in many cases does not exist, has not been
74 recorded continuously or for sufficient duration (Acreman and Dunbar, 2004). To speed up
75 ecological reserve determination, river flow records have been used to analyse natural
76 seasonality and variability of flows (e.g. Hughes and Hannart, 2003). However, this approach
77 requires long-term streamflow and baseflow timeseries. Whilst streamflow is a measurable
78 quantity subject to a gauging station being in place, baseflow has to be modelled based on
79 hydrological and hydrogeological variables.

80 While rainfall/runoff models can be used to calculate hydrological variables using distributive
81 surface water components (e.g. J2000: Krause, 2001), groundwater variables are lumped within
82 the modelling framework. In contrast, groundwater models which distribute groundwater
83 variables (e.g. MODFLOW: Harbaugh, Arlen, 2005), are frequently setup to lump climate
84 components. In order to accurately model daily baseflow, which is needed for ecological
85 reserve determination, modelling systems need to be setup such that both groundwater and
86 climate variables are treated in a distributive manner (e.g. Kim et al., 2008). Rainfall/runoff
87 models which use Hydrological Response Units (HRUs) as an entity of homogenous climate,
88 rainfall, soil and landuse properties (Flügel, 1995) are able to reproduce hydrographs through
89 model calibration (Wagener and Wheater, 2006). However, they are rarely able to correctly
90 proportion runoff and baseflow components (e.g. Robson et al., 1992). To correctly determine
91 groundwater baseflow using rainfall/runoff models such as the J2000, aquifer components need
92 to be distributed. This can be achieved using net recharge and hydraulic conductivity collected
93 through aquifer testing or groundwater model values.



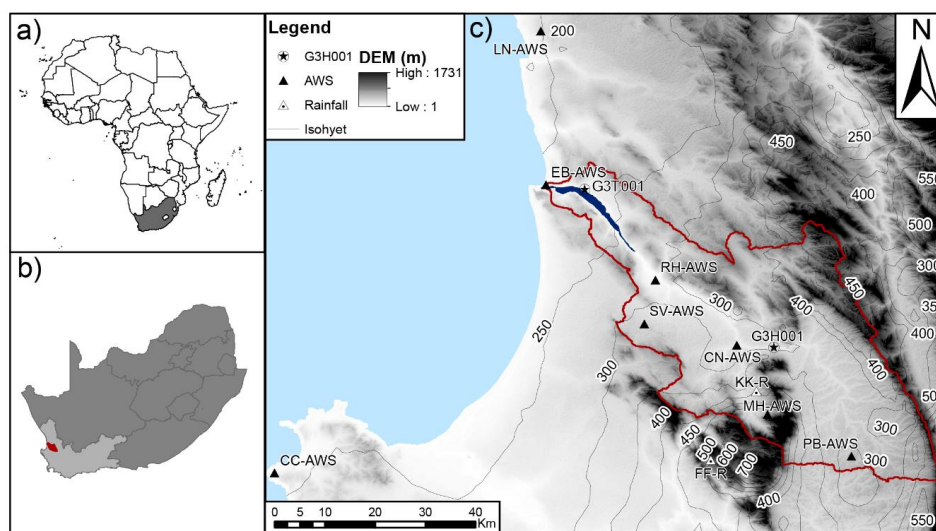
94 To better understand the nature of river flow regime dynamics, a J2000 rainfall/runoff model
95 previously setup to simulate surface water processes (Watson et al., 2018) was distributed to
96 incorporate aquifer hydraulic conductivity within model HRUs using calibrated values from a
97 groundwater model (Watson, submitted). The model was setup for the RAMSAR listed
98 Verlorenvlei estuarine system on the west coast of South Africa, which is under threat from
99 climate change and agricultural expansion. While the estuarine lake's importance is well
100 documented (Martens et al., 1996; Wishart, 2000), the ecological reserves of the main feeding
101 tributaries have not yet been set, partially due to a lack of streamflow and baseflow estimates
102 within the sub-catchment. The modelling framework developed in this study aimed to provide
103 the hydrological components, (baseflow and runoff proportioning) of the tributaries needed to
104 set the ecological reserve. The surface water and groundwater components of the model were
105 calibrated for two different tributaries which were believed to be the main source of runoff and
106 baseflow for the sub-catchment. The baseflow and runoff rates calculated from the model
107 indicate not only that the lake system cannot be sustained by baseflow during low flow periods
108 but also that the initial understanding of which tributaries are key to the sustainability of the
109 lake system was not correct. The results have important implications for how we understand
110 water dynamics in water stressed catchments and the sustainability of ecological systems in
111 these environments.

112 **2. Study site**

113 Verlorenvlei is an estuarine lake situated on the west coast of South Africa, approximately 150
114 km north of the metropolitan city of Cape Town (Fig. 1). The west coast, which is situated in
115 the Western Cape Province of South Africa, is subject to a Mediterranean climate where the
116 majority of rainfall is received between May to September. The Verlorenvlei lake, which is
117 approximately 15 km² in size draining a watershed of 1832 km², forms the southern sub-



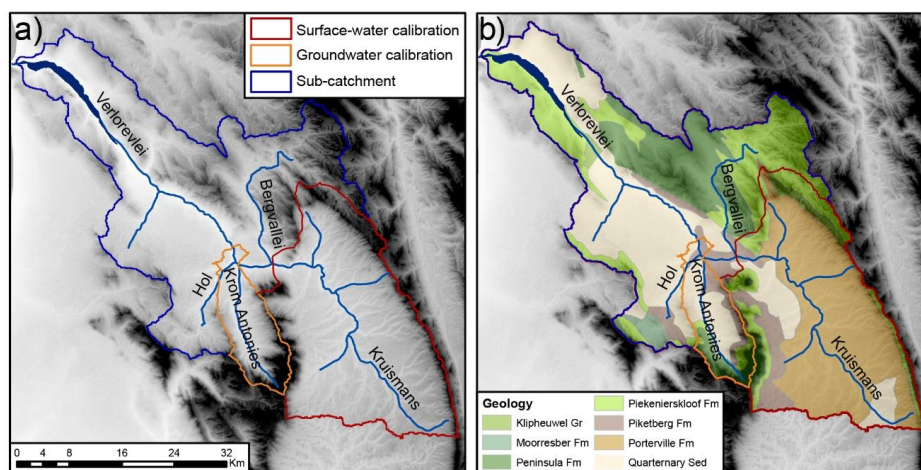
118 catchment of the Olifants/Doorn quaternary catchment. The estuarine lake supports both
119 Karroid and Fynbos biomes, due to the intermittent connection between salt and fresh water.
120 A sandbar created around a sandstone outcrop (Table Mountain Group) allows for freshwater
121 to exit the lake to the sea, as well as reducing sea water flow within the lake. The lake is
122 supplied by four main tributaries which are the Krom Antonies, Bergvallei, Hol and Kruismans.
123 The main freshwater sources are suggested to be the Krom Antonies (Sigidi, 2018) and the
124 Bergvallei, which drain the mountainous regions to the south (Piketberg) and north of the sub-
125 catchment respectively. The Hol and Kruismans tributaries are variably saline (Sigidi, 2018),
126 due to high evaporation rates in the valley. Average daily temperatures during summer within
127 the sub-catchment are between 20-30 °C, with estimated potential evaporation rates of 4 to 6
128 mm.d⁻¹ (Muche et al., 2018). In comparison, winter daily average temperatures are between 12-
129 20 °C, with estimated potential evaporation rates of 1 to 3 mm.d⁻¹ (Muche et al., 2018).



130
131 Figure 1: a) Location of South Africa, b) the location of the study catchment within the Western
132 Cape and c) the extend of the Verlorenvlei sub-catchment with the climate stations, gauging
133 station (G3H001), measured lake water level (G3T001) and rainfall isohets



134 The sub-catchment is comprised of three main lithological units, namely: 1) quaternary
135 sediments 2) Table Mountain Group (TMG) sandstones and 3) Malmesbury (MG) shales (Fig
136 2). The quaternary sediments make up the primary aquifer within the sub-catchment, while the
137 TMG sandstones and MG shales make up the secondary aquifer. The catchment valley, which
138 receives the least mean annual precipitation (MAP) (150-500 mm.year⁻¹: Lynch, 2004), is
139 comprised of quaternary sediments that vary in texture, although the majority of the sediments
140 in the sub-catchment are sandy in nature. The higher relief mountainous regions of the sub-
141 catchment, which receive the highest MAP (550-1000 mm.year⁻¹: Lynch, 2004), are mainly
142 comprised of fractured TMG sandstones, (youngest to oldest): Peninsula, Graafwater (not
143 shown), and Piekernerskloof formations (Fig. 2). Underlying the sandstones and quaternary
144 sediments are the MG shales, which are comprised of the Mooresberg, Piketberg and
145 Klipheuwel formations (Fig. 2). The MG shales and quaternary sediments which host the
146 secondary and primary aquifer respectfully, are frequently used to supplement irrigation during
147 the summer months of the year. During winter, the majority of the irrigation water needed for
148 crop growth is supplied by the sub-catchment tributaries or lake itself. Agriculture is the
149 dominant water user in the sub-catchment with an estimated usage of 20 % of the total recharge
150 (DWAF, 2003; Watson *et al.*, submitted), with the main food crop being potatoes. For further
151 information regarding the study site refer to Watson *et al.*, (2018).

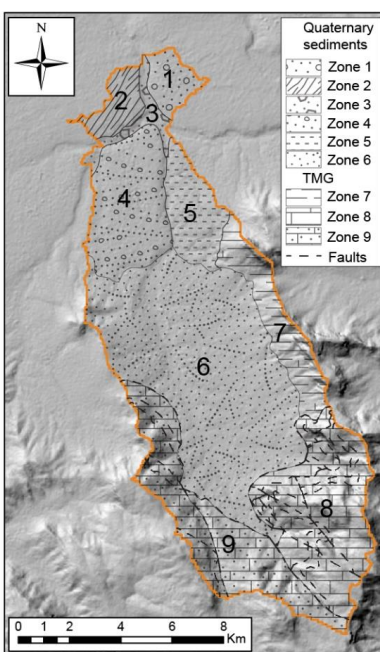


152

153 Figure 2: a) The Verlorenvlei sub-catchment with the surface water calibration tributary
154 (Kruismans) and groundwater calibration tributary (Krom Antonies) and b) the hydrogeology
155 of the sub-catchment with Malmesbury shale formations (Klipheuwel, Mooresberg, Porterville,
156 Piketberg), Table Mountain Group formations (Peninsula, Piekenierskloof) and quaternary
157 sediments

158 3. Methodology

159 For this study, the J2000 coding was adapted to incorporate distributive groundwater
160 components. To do this, the hydraulic conductivity or maximum percolation value for specific
161 geological formations was assigned to the model HRU's, using net recharge and calibrated
162 aquifer hydraulic conductivity from a groundwater model (Watson, submitted) determined for
163 eight hydraulic zones (Fig. 3). The adaption was applied to the groundwater components of the
164 J2000 coding which influenced the portioning of water routed to runoff and baseflow. To
165 validate the outputs of the model, an empirical mode decomposition (EMD) (Huang et al.,
166 1998) was applied to compute the proportion of variation in discharge timeseries that attributed
167 to a high and low water level change at the sub-catchment outlet.



168

169 Figure 3: The aquifer hydraulic zones used for the groundwater calibration of the J2000 (after
170 Watson, submitted)

171 3.1 Hydrological Response Unit Delineation

172 HRUs and stream segments (reaches) are used within the J2000 model for distributive
173 topographic and physiological modelling. In this study, the HRU delineation made use of a
174 digital elevation model, with slope, aspect, solar radiation index, mass balance index and
175 topographic wetness being derived. Before the delineation process, gaps within the digital
176 elevation model were filled using a standard fill algorithm from ArcInfo (Jenson and
177 Domingue, 1988). The AML (ArcMarkupLanguage) automated tool (Pfennig et al., 2009) was
178 used for the HRU delineation, with between 13 and 14 HRUs/km² being defined
179 (Pfannschmidt, 2008). After the delineation of HRUs, dominant soil, land use and geology
180 properties were assigned to each. The hydrological topology was defined for each HRU by
181 identifying the adjacent HRUs or stream segments that received water fluxes.



182 **3.2 Model regionalisation**

183 Rainfall and relative humidity are the two main parameters that are regionalised within the
184 J2000 rainfall/runoff model. While a direct regionalisation using an inverse-distance method
185 (IDW) and the elevation of each HRU can be applied to rainfall data, the regionalisation of
186 relative humidity requires the calculation of absolute humidity. The regionalisation of rainfall
187 records was applied by defining the number of weather station records available and estimating
188 the influence on the rainfall amount for each HRU. A weighting for each station using the
189 distance of each station to the area of interest was applied to each rainfall record, using an
190 elevation correction factor (Watson et al., 2018). The relative humidity and air temperature
191 measured at set weather stations was used to calculate the absolute humidity. Absolute
192 humidity was thereafter regionalised using the IDW method, station and HRU elevation. After
193 the regionalisation had been applied, the absolute humidity was converted back to relative
194 humidity through calculation of saturated vapor pressure and the maximum humidity.

195 **3.3 Water balance calculations**

196 The J2000 model is divided into calculations that impact surface water and groundwater
197 processors. The J2000 model distributes the regionalised precipitation (P) calculated for each
198 HRU using a water balance defined as:

$$P = R + Int_{max} + ETR + \Delta Soil_{sat} \quad (1)$$

199 where R is runoff (mm) (RD1 - surface runoff; RD2 - interflow), Int_{max} is vegetation canopy
200 interception (mm), ETR is 'real' evapotranspiration and $\Delta Soil_{sat}$ is change in soil saturation.
201 The surface water processes have an impact on the amount of modelled runoff and interflow,
202 while the groundwater processors influence the upper and lower groundwater flow
203 components.

204 **3.3.1 Surface water components**

205 Potential evaporation (ETP) within the J2000 model is calculated using the Penman Monteith
206 equation. Before evaporation was calculated for each HRU, interception was subtracted from
207 precipitation using the leaf area index and leaf storage capacity for vegetation (a_{rain})
208 (Supplementary: Table 1). Evaporation within the model considers several variables that
209 influence the overall modelled evaporation. Firstly, evaporation is influenced by a slope factor,
210 which was used to reduce ETP based on a linear function. Secondly, the model assumed that
211 vegetation transpires until a particular soil moisture content where ETP is reached, after which
212 modelled evaporation was reduced proportionally to the ETP, until it became zero at the
213 permanent wilting point.

214 The soil module in the J2000 model is divided up into processing and storage units. Processing
215 units in the soil module include soil-water infiltration and evapotranspiration, while storage
216 units include middle pore storage (MPS), large pore storage (LPS) and depression storage. The
217 infiltrated precipitation was calculated using the relative saturation of the soil, and its maximum
218 infiltration rate ($SoilMaxInfSummer$ and $SoilMaxInfWinter$) (Supplementary: Table 1).
219 Surface runoff was generated when the maximum infiltration threshold was exceeded. The
220 amount of water leaving LPS, which can contribute to recharge, was dependant on soil
221 saturation and the filling of LPS via infiltrated precipitation. Net recharge (R_{net}) was estimated
222 using the hydraulic conductivity ($SoilMaxPerc$), the outflow from LPS (LPS_{out}) and the slope
223 ($slope$) of the HRU according to:

$$R_{net} = LPS_{out} \times (1 - \tan(slope) SoilMaxPerc) \quad (2)$$

224 The hydraulic conductivity, $SoilMaxPerc$ and the adjusted LPS_{out} were thereafter used to
225 calculate interflow (IT_f) according to:



$$IT_f = LPS_{out} \times (\tan(\text{slope}) \text{ SoilMaxPerc}) \quad (3)$$

226 with the interflow calculated representing the sub-surface runoff component RD2 and is routed
 227 as runoff within the model.

228 3.3.2 Groundwater components

229 The J2000 model for the Verlorenvlei sub-catchment was set up with two different geological
 230 reservoirs: (1) the primary aquifer (upper groundwater reservoir - RG1), which consists of
 231 quaternary sediments with a high permeability; and (2) the secondary aquifer (lower
 232 groundwater reservoir- RG2), made up of MG shales and TMG sandstones (Table 1).

Aquifer	Formation	Type	RG1_max (mm)	RG2_max (mm)	RG1_k (d)	RG2_k (d)	RG1_active (n/a)	Kf_geo (mm/d)	depthRG1 (cm)
Primary	Quaternary Sediments	Sediments	50	700	100	431	1	500	1750
Secondary/MG	Moorresberg Formation	Shale Greywacke	0	580	0	350	0	950	1750
Secondary/MG	Porterville Formation	Shale Greywacke	0	560	0	335	0	2	1750
Secondary/MG	Piketberg Formation	Shale Greywacke	0	1000	0	600	0	950	1750
Secondary/MG	Klipheuwel Group	Shale Greywacke	0	500	0	300	0	950	1750
Secondary/TMG	Peninsula Formation	Sandstone	0	1000	0	600	0	950	1750
Secondary/TMG	Piekenierskloof Formation	Sandstone	0	600	0	400	0	1	1750

233

234 Table 1: The J2000 hydrogeological parameters RG1_max, RG2_max, RG1_k, RG2_Kf_geo
 235 and depthRG1 assigned to the primary and secondary aquifer formations for the Verlorenvlei
 236 sub-catchment

237 The model therefore considered two baseflow components, a fast one from the RG1 and a
 238 slower one from RG2. The filling of the groundwater reservoirs was done by net recharge, with
 239 emptying of the reservoirs possible by lateral subterranean runoff as well as capillary action in
 240 the unsaturated zone. Each groundwater reservoir was parameterised separately using the
 241 maximum storage capacity (maxRG1 and maxRG2) and the retention coefficients for each
 242 reservoir (*recRG1* and *recRG2*). The outflow from the reservoirs was determined as a function
 243 of the actual filling (*actRG1* and *actRG2*) of the reservoirs and a linear drain function.
 244 Calibration parameters *recRG1* and *recRG2* are storage residence time parameters. The
 245 outflow from each reservoir was defined as:



$$OutRG1 = \frac{1}{gwRG1Fact \times recRG1} \times actRG1 \quad (4)$$

$$OutRG2 = \frac{1}{gwRG2Fact \times recRG2} \times actRG2 \quad (5)$$

246 where $OutRG1$ is the outflow from the upper reservoir, $OutRG2$ is the outflow from the lower
 247 reservoir and $gwRG1Fact/gwRG2Fact$ are calibration parameters for the upper and lower
 248 reservoir used to determine the outflow from each reservoir. To allocate the quantity of net
 249 recharge between the upper (RG1) and lower (RG2) groundwater reservoirs, a calibration
 250 coefficient $gwRG1RG2sdist$ was used to distribute the net recharge for each HRU using the
 251 HRU slope. The influx of groundwater into the shallow reservoir ($inRG1$) was defined as:

$$inRG1 = R_{net} \times (1 - (1 - \tan(slope))) \times gwRG1RG2sdist \quad (6)$$

252 The influx of net recharge into the lower groundwater reservoir ($inRG2$) was defined as:

$$inRG2 = R_{net} \times (1 - \tan(slope)) \times gwRG1RG2sdist \quad (7)$$

253 with the combination of $OutRG1$ and $OutRG2$ representing the baseflow component that is
 254 routed as an outflow from the model.

255 3.4 Lateral and reach routing

256 Lateral routing was responsible for water transfer within the model and included HRU influxes
 257 and discharge through routing of cascading HRUs from the upper catchment to the exit stream.
 258 HRUs were either able to drain into multiple receiving HRUs or into reach segments, where
 259 the topographic ID within the HRU dataset determined the drain order. The reach routing
 260 module was used to determine the flow within the channels of the river using the kinematic
 261 wave equation and calculations of flow according to Manning and Strickler. The river
 262 discharge was determined using the roughness coefficient of the stream (Manning roughness),
 263 the slope and width of the river channel and calculations of flow velocity and hydraulic radius
 264 calculated during model simulations.



265 **4.1 J2000 Input data**

266 After the above adaptations of the J2000 model coding, input data representing both the surface
267 water and groundwater components were required.

268 **4.1.1 Surface water components**

269 Climate and rainfall: Rainfall, windspeed, relative humidity, solar radiation and air temperature
270 were monitored by Automated Weather Stations (AWS) within and outside of the study
271 catchment (Fig. 1). Of the climate and rainfall data used during the surface water modelling
272 (Watson et al., 2018), data was sourced from six AWS's of which four stations were owned by
273 the South African Weather Service (SAWS) and three by the Agricultural Research Council
274 (ARC). Two stations that were installed for the surface water modelling, namely Moutonshoek
275 (M-AWS) and Confluence (CN-AWS) were used for climate and rainfall validation due to their
276 short record length. Additional rainfall data collected by farmers at high elevation at location
277 FF-R and within the middle of the catchment at KK-R were used to improve the climate and
278 rainfall network density.

279 Landuse classification: The vegetation and landuse dataset that was used for the sub-catchment
280 (CSIR, 2009) included five different landuse classes: 1) wetlands and waterbodies, 2)
281 cultivated (temporary, commercial, dryland), 3) shrubland and low fynbos, 4) thicket,
282 bushveld, bush clumps and high fynbos and 5) cultivated (permanent, commercial, irrigated).
283 Each different landuse class was assigned an albedo, root depth and seal grade value based on
284 previous studies (Steudel et al., 2015)(Supplementary: Table 2). The Leaf Area Index (LAI)
285 and vegetation height varies by growing season with different values of each for the particular
286 growing season. While surface resistance of the landuse varied monthly within the model, the
287 values only vary significantly between growing seasons.



288 Soil dataset: The Harmonized World Soil Database (HWSD) v1.2 (Batjes et al., 2012) was the
289 input soil dataset, with nine different soil forms within the sub-catchment (Supplementary:
290 Table 3). Within the HWSD, soil depth, soil texture and granulometry were used to calculate
291 and assign soil parameters within the J2000 model. MPS and LPS which differ in terms of the
292 soil structure and pore size were determined in Watson et al. (2018), using pedotransfer
293 functions within the HYDRUS model (Supplementary: Table 3).

294 Streamflow and water levels: Streamflow, measured at the Department of Water Affairs
295 (DWA) gauging station G3H001 between 1970-2009, at the outlet of the Kruismans tributary
296 (Het Kruis) (Fig 1 and 2), was used for surface water calibration. The G3H001 two-stage weir
297 could record a maximum flow rate of $3.675 \text{ m}^2 \cdot \text{s}^{-1}$ due to the capacity limitations of the
298 structure. After 2009, the G3H001 structure was decommissioned due to structural damage,
299 although repairs are expected in the near future due to increasing concerns regarding the influx
300 of freshwater into the lake. Water levels measured at the sub-catchment outlet at DWA station
301 G3T001 (Fig 1) between 1994 to 2018 were used for EMD filtering.

302 ***4.1.2 Groundwater components***

303 Net recharge and hydraulic conductivity: The net recharge and hydraulic conductivity values
304 used for the groundwater model calibration were collected from detailed MODFLOW
305 modelling conducted for the Krom Antonies tributary (Fig. 3) (Watson, submitted). The net
306 recharge and aquifer hydraulic conductivity for the Krom Antonies tributary, was estimated
307 through PEST autocalibration using hydraulic conductivities from previous studies (SRK,
308 2009; UMVOTO-SRK, 2000) and potential recharge estimates (Watson et al., 2018).

309 Hydrogeology: Within the hydrogeological dataset, parameters assigned include maximum
310 storage capacity (RG1 and RG2), storage coefficients (RG1 and RG2), the minimum
311 permeability/maximum percolation (K_{f_geo} of RG1 and RG2) and depth of the upper



312 groundwater reservoir (depthRG1). The maximum storage capacity was determined using an
313 average thickness of each aquifer and the total number of voids and cavities, where the primary
314 aquifer thickness was assumed to be between 15-20 m (Conrad et al., 2004), and the secondary
315 aquifer between 80-200 m (SRK, 2009). The maximum percolation of the different geological
316 formations was assigned hydraulic conductivities using the groundwater model for the Krom
317 Antonies sub-catchment (Watson et al., submitted). The J2000 geological formations were
318 assigned conductivities to modify the maximum percolation value to ensure internal
319 consistency with recharge values calculated using MODFLOW (Table 1).

320 **4.2 Model calibration**

321 **4.2.1 Model sensitivity**

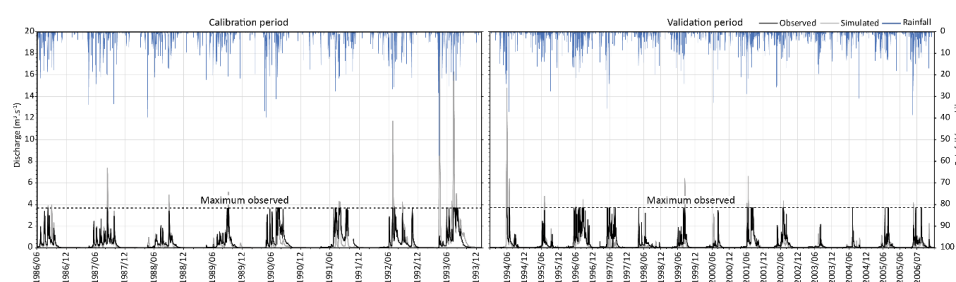
322 The J2000 sensitivity analysis for Verlorenvlei sub-catchment was presented in Watson *et al.*,
323 (2018) and therefore only a short summary is presented here. In this study, parameters that
324 were used to control the ratio of interflow to percolation were adjusted, which in the J2000
325 model include a slope (SoilLatVertDist) and max percolation value. The sensitivity analysis
326 conducted by Watson *et al.*, (2018) showed that for high flow conditions (E2) (Nash-Sutcliffe
327 efficiency in its standard squared), model outputs are most sensitive to the slope factor, while
328 for low flow conditions (E1) (modified Nash-Sutcliffe efficiency in a linear form) the model
329 outputs were most sensitive to the maximum infiltration rate of the soil (ie. the parameter
330 maxInfiltrationWet) (Supplementary: Figure 1). The max percolation was moderately sensitive
331 during wet and dry conditions, and together with the slope factor, controlled the interflow to
332 percolation portioning that was calibrated in this study.

333 **4.2.2 Surface water calibration**

334 The surface water parameters of the model were calibrated for the Kruismans tributary (688
335 km²) (Fig. 2) using the gauging data from G3H001 (Fig. 4 and Table 1). The streamflow data



336 used for the calibration was between 1986-1993, with model validation between 1994 to 2007
337 (Fig. 4). This specific calibration period was selected due to the wide range of different runoff
338 conditions experienced at the station, with both low and high flow events being recorded. For
339 the calibration, the modelled discharge was manipulated in the same fashion, with a maximum
340 value of 3.675 m³/s, so that the tributary streamflow behaved as measured discharge.



341

342 Figure 4: The surface water calibration (1986-1993) and validation (1986-2006) of the J2000
343 model using gauging data from the G3H001

344 An automated model calibration was performed using the “Nondominating Sorting Genetic
345 Algorithm II” (NSGA-II) multi-objective optimisation method (Deb et al., 2002) with 1023
346 model runs being performed. Narrow ranges of calibration parameters (FC_Adaptation,
347 AC_Adaptation, soilMAXDPS, gwRG1Fact and gwRG2Fact) were chosen to (1) ensure that
348 the modelled recharge from J2000 was within an order of magnitude of recharge from the
349 MODFLOW model; (2) to achieve a representative sub-catchment hydrograph. As objective
350 functions, the E2, E1 and the average bias in % (Pbias) were utilized for the calibration (Krause
351 et al., 2005) (Table 2). The choice of the optimized parameter set was made to ensure that E2
352 was better than 0.57 (best value was 0.574302) and the Pbias better than 5% (Table 1). From
353 the automated calibration, 308 parameter sets were determined with the best E1 being chosen
354 to ensure that the model is representative of low flow conditions (Table 1).

355 **4.2.3 Model validation**

356 For the surface water model validation, the streamflow records between 1994-2007 were used,
 357 where absolute values (E1) and squared differences (E2) of the Nash Sutcliffe efficiency were
 358 reported. The Pbias was also used as an objective function to report the model performance by
 359 comparison between measured and modelled streamflow (Table 2). Although gauging station
 360 limitations resulted in good objective functions from the model, the performance of objective
 361 functions E1, E2, Pbias reduced between the validation and calibration period (Table 2). During
 362 the calibration period there was a good fit between modelled and measured streamflow (Pbias=
 363 1.82), with a significant difference between modelled and measured streamflow during the
 364 validation period (Pbias=-19.2). The calibration was performed over a wet cycle (1986-1997),
 365 which resulted in a more common occurrence of streamflow events that exceeded $3.675 \text{ m}^3 \cdot \text{s}^{-1}$
 366 ¹, thereby reducing the number of calibration points. In contrast the validation was performed
 367 over a dry cycle (1997-2007), which resulted in more data points as few streamflow events
 368 exceeded $3.675 \text{ m}^3 \cdot \text{s}^{-1}$.

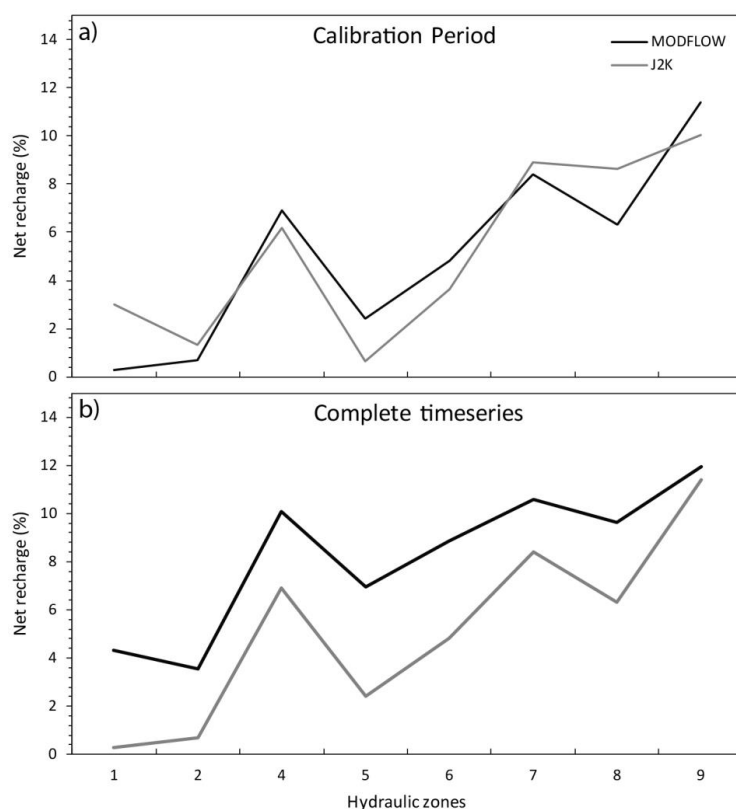
	Calibration:	Validation:
	1987-1993	1994-2007
e1	0.55085	0.53312
e2	0.57156	0.55736
R ²	0.61788	0.58067
Pbias	-1.82301	-19.23758

369
 370 Table 2: The objective functions E1, E2, coefficient of determination R² and Pbias used for the
 371 surface water calibration (1987-1993) and validation (1987-2007)

372 The groundwater recharge values from MODFLOW were validated with J2000 recharge
 373 estimates (Fig. 5). During the calibration period the groundwater recharge proportion for the
 374 eight calibrated hydraulic zones (Fig. 3) achieved a good fit, with an average value from J2000
 375 of 4.71 % and from MODFLOW of 4.58 %. The coefficient of determination (R²) between the



376 J2000 and MODFLOW was 0.81. Across the entire dataset J2000 overestimates groundwater
377 recharge by 2.75 %, although the coefficient of determination produced an R^2 of 0.92 which is
378 higher than the calibration period.



379

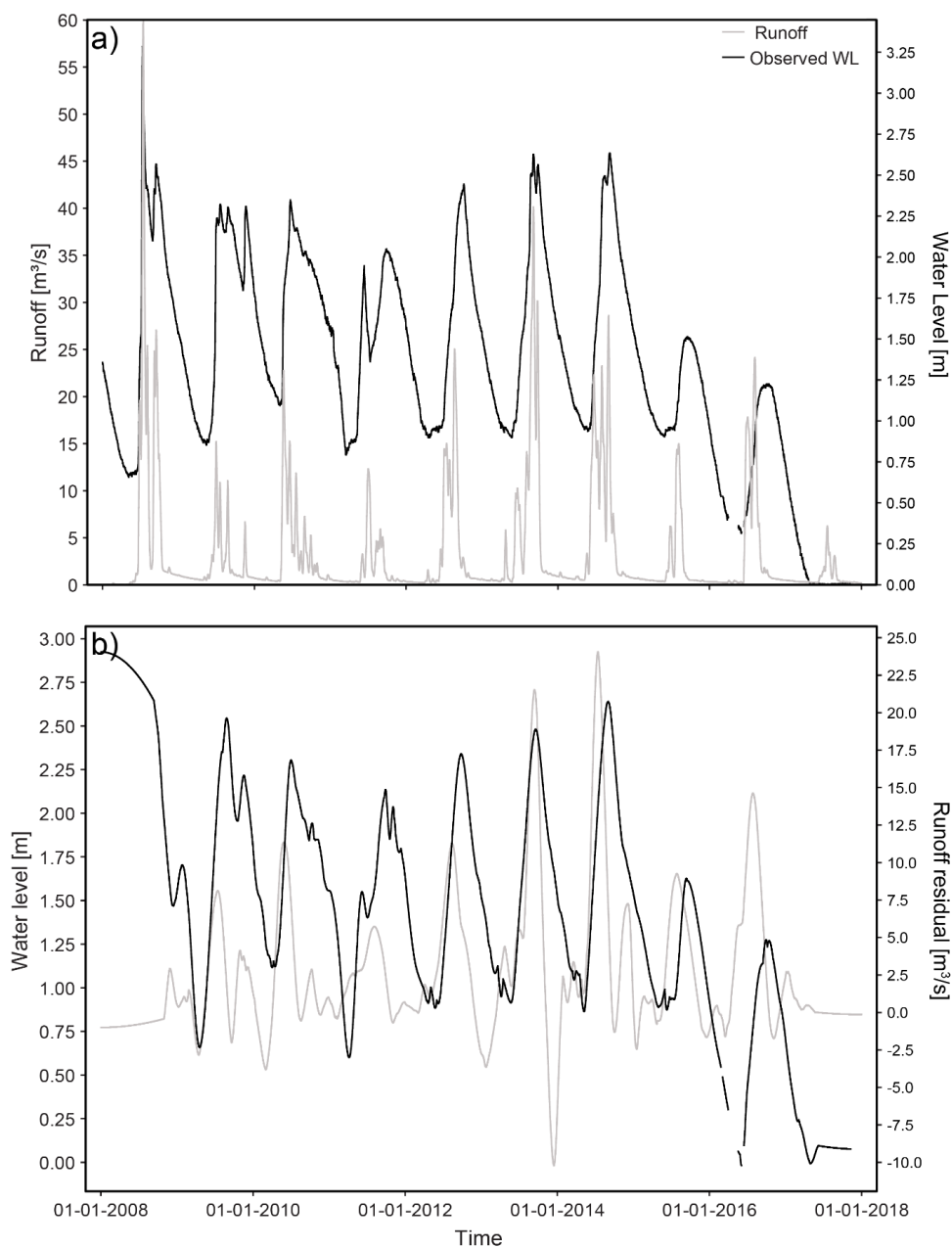
380 Figure 5: The groundwater calibration for each hydraulic zone with a) net recharge for the
381 J2000 and MODFLOW during the model calibration (2016) and b) the net recharge deviation
382 between MODFLOW and J2000 across the entire modelling timestep (1986-2017)

383 4.3 EMD filtering

384 To account for missing streamflow data between 2007-2017, an Empirical Mode
385 Decomposition (EMD) (Huang et al., 1998) was applied to the measured water level data at
386 the sub-catchment outlet (G3T001)(Fig. 1) between 1994 to 2018 (Fig 6a). EMD is a method



387 for the decomposition of nonlinear and nonstationary signals into sub-signals of varying
388 frequency, so-called intrinsic mode functions (IMF), and a residuum signal. By removing one
389 or more IMF or the residuum signal, certain frequencies (e.g. noise) or an underlying trend can
390 be removed from the original time series data. This approach was successfully applied to the
391 analysis of river runoff data (Huang et al., 2009) and forecasting of hydrological time series
392 (Kisi et al., 2014). In this study, EMD filtering was used to remove high frequency sub-signals
393 from simulated runoff and measured water level data to compare the more general seasonal
394 variations of both signals (Fig. 6b).



395

396 Figure 6: a) The water level fluctuations at station G3T001 with modelled runoff and b) the
397 EMD filtering showing the variation in discharge timeseries attributed a water level change at
398 the station



399 **5. Results**

400 The J2000 model was used to simulate both runoff and baseflow, with runoff being comprised
401 of direct surface runoff (RD1) and interflow (RD2) and baseflow simulated from the primary
402 (RG1) and secondary aquifer (RG2). Below, the results of the modelled streamflow and
403 baseflow are presented, along with the total flow contribution of each tributary, the runoff to
404 baseflow proportioning and stream exceedance probabilities. The coefficient of variation (CV)
405 was used to determine the streamflow variability of each tributary, while the baseflow index
406 (BFI) was used to determine the baseflow and runoff proportion.

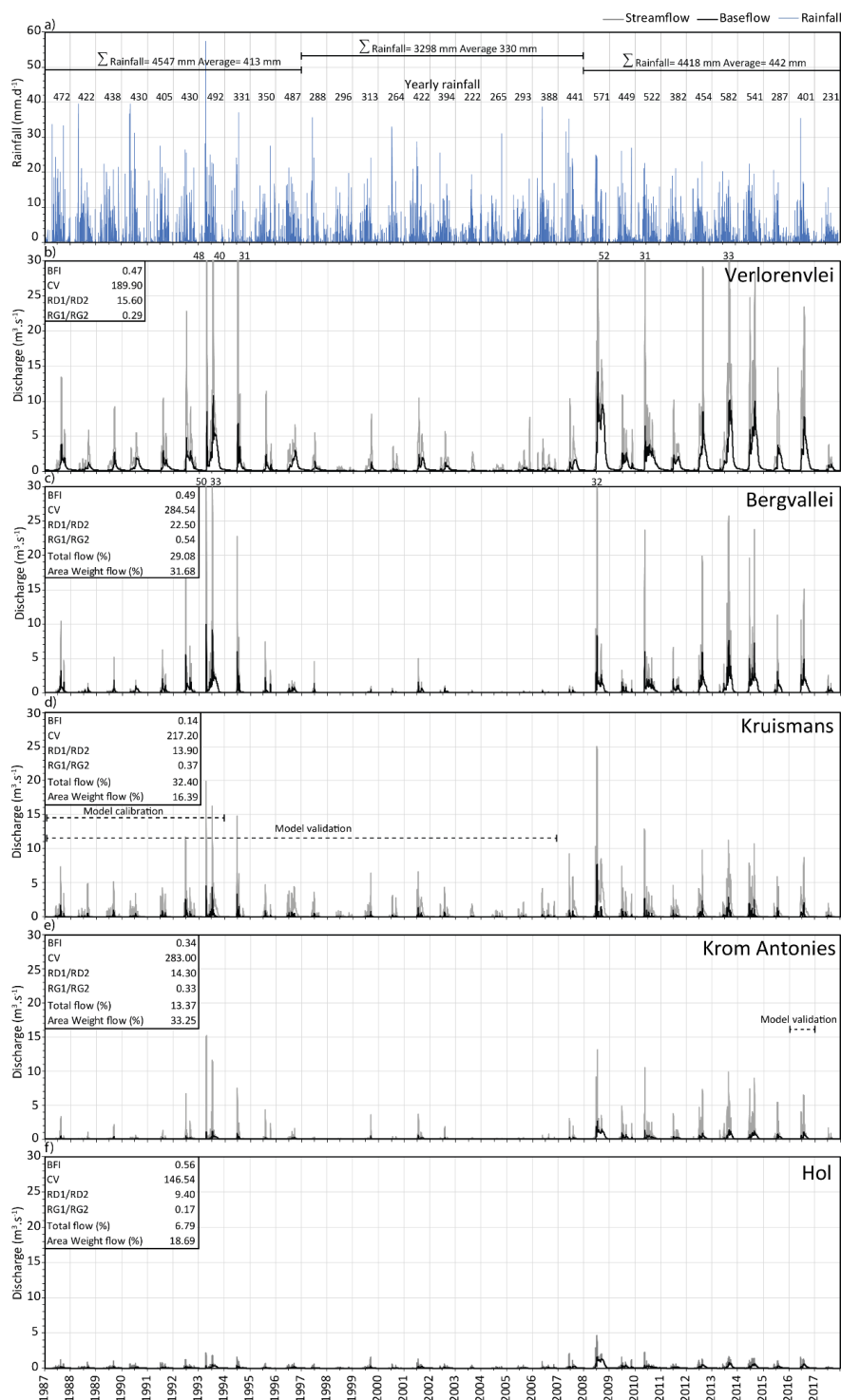
407 **5.1 Streamflow and baseflow**

408 Streamflow for the sub-catchment shows two distinctively wet periods (1987-1997 and 2007-
409 2017), separated by a dry period (1997-2007) (Fig. 7). Yearly sub-catchment rainfall volumes
410 between 1987-1997 were between 288 and 492 mm/yr⁻¹, with an average of 404 mm.yr⁻¹. For
411 this period, average yearly streamflow between 1987-1997 was 1.4 m³.s⁻¹, with an average
412 baseflow contribution of 0.63 m³.s⁻¹. The modelled streamflow reached a maximum of 48 m³.s⁻¹
413 in 1993, when 5 m³.s⁻¹ of baseflow was generated after 58 mm of rainfall was received.
414 Between 1997-2007 (dry period) sub-catchment yearly rainfall was between 222 and 394
415 mm/yr⁻¹ with an average of 330 mm.yr⁻¹ (Fig. 7). For this period, average yearly streamflow
416 between 1997-2007 was 0.44 m³.s⁻¹, with an average baseflow contribution of 0.18 m³.s⁻¹. The
417 modelled streamflow reached a maximum of 11 m³.s⁻¹ in 2002, with a baseflow contribution
418 of 2.5 m³.s⁻¹ after 28 mm of rainfall was received. Between 2007-2017 (wet period) sub-
419 catchment yearly rainfall was between 231 and 582 mm.yr⁻¹ with an average of 427 mm.yr⁻¹
420 (Fig. 7). Over this period, average yearly streamflow between 2007-2017 was 2.5 m³.s⁻¹ with
421 an average baseflow contribution of 1.3 m³.s⁻¹. The modelled streamflow reached a maximum



422 of $52 \text{ m}^3 \cdot \text{s}^{-1}$ in 2008, with $13 \text{ m}^3 \cdot \text{s}^{-1}$ of baseflow generated after two consecutive rainfall events

423 each of 25 mm.





425 Figure 7: a) The average sub-catchment rainfall between 1987-2017 showing wet cycles (1987-
426 1997 and 2008-2017), the modelled streamflow and baseflow inflows for the b) Verlorenvlei,
427 c) Bergvallei, d) Kruismans, e) Krom Antonies and f) Hol with estimated BFI, CV, RD1/RD2,
428 RG1/RG2

429 **5.2 Tributary contributions**

430 The four main feeding tributaries (Bergvallei, Kruismans, Hol and Krom Antonies) together
431 contribute 81% of streamflow for the Verlorenvlei, with the additional 19% from small
432 tributaries near Redelinghuys (Fig. 7). The Kruismans contributes most of the total streamflow
433 with 32.4 %, although due to the sub-catchment being the largest of the tributaries (688 km²),
434 the area weighted contribution is 16.4 % (Fig. 7). The Bergvallei (320 km²), which is smaller
435 than the Kruismans, contributes 29 % of the total flow with an area weighted contribution of
436 32 %. The Krom Antonies has the largest area weighted contribution of 33 % due to its small
437 size (140 km²) in comparison to the other tributaries, although the Krom Antonies contributes
438 only 13 % of the total flow (Fig. 7). The Hol (126 km²) contributes the least total flow with
439 6.79 %, with a weighted contribution of 18.69 % (Fig. 7).

440 **5.3 Flow variability**

441 Streamflow that enters Verlorenvlei has a large daily variability with a coefficient of variation
442 of 189.90 (Fig. 7). Verlorenvlei's streamflow is mainly comprised of surface runoff
443 (RD1/RD2=15.6) as opposed to interflow. The total groundwater flow contribution for the
444 Verlorenvlei is 47 % (BFI=0.47) with the majority of groundwater baseflow from the
445 secondary aquifer (RG1/RG2=0.29). The Kruismans has large daily streamflow variability
446 with a CV of 217.20 (Fig. 7). The Kruismans tributary is mainly comprised of surface runoff
447 (RD1/RD2=13.9) with a small interflow contribution. The total groundwater flow contribution
448 for the Kruismans tributary is relatively low, with groundwater making up 14 % of streamflow



449 (BFI=0.14), where the majority of baseflow is from the secondary aquifer (RG1/RG2=0.37).
450 The Bergvallei has the highest streamflow variability, with a CV of 284.54, and the highest
451 surface runoff to interflow proportion (RD1/RD2=22.50), with a total groundwater
452 contribution of 49 % (BFI=0.49) (Fig. 7). The secondary aquifer contributes the majority of
453 baseflow for the Bergvallei, with the secondary aquifer contribution being more than double
454 the primary aquifer (RG1/RG2=0.54). The Krom Antonies has significant variability in daily
455 streamflow, with a CV of 283.00 (Fig. 7). The runoff from the Krom Antonies is mainly
456 comprised of surface runoff with interflow being a minor contribution (RD1/RD2=14.30). The
457 Krom Antonies has a relatively high groundwater component (BFI=0.34), with the secondary
458 aquifer contributing the most baseflow (RG1/RG2=0.33). The Hol tributary has the lowest
459 variability in daily streamflow with a CV of 146.54 (Fig. 7). The Hol tributary is mainly
460 comprised of surface runoff (RD1/RD2=9.40), although the interflow is the highest proportion
461 within the sub-catchment. The Hol tributary is mainly comprised of groundwater (BFI=0.56),
462 with the majority of baseflow being derived from the secondary aquifer (RG1/RG2=0.17).

463 **5.4 Flow exceedance probabilities**

464 The results for the flow exceedance probabilities includes flow volumes for each tributary and
465 the lake's inflow which are exceeded 95%, 75%, 50%, 25 and 5 % of the time. The 95 percentile
466 corresponds to a lake inflow of $0.054 \text{ m}^3 \cdot \text{s}^{-1}$ or $4,702 \text{ m}^3 \cdot \text{d}^{-1}$, with between $0.001\text{-}0.004 \text{ m}^3 \cdot \text{s}^{-1}$
467 from the feeding tributaries (Table 3). The 75-percentile flow, which is exceeded 3/4 of the
468 time corresponds to an inflow of $0.119 \text{ m}^3 \cdot \text{s}^{-1}$ or $10,303 \text{ m}^3 \cdot \text{d}^{-1}$, with between $0.005\text{-}0.015 \text{ m}^3 \cdot \text{s}^{-1}$
469 from the feeding tributaries. Average (50 percentile) streamflow flowing into the Verlorenvlei
470 is $0.237 \text{ m}^3 \cdot \text{s}^{-1}$ or $20,498 \text{ m}^3 \cdot \text{d}^{-1}$, with between $0.012\text{-}0.012 \text{ m}^3 \cdot \text{s}^{-1}$ from the feeding tributaries.
471 The 25-percentile flow, which is exceeded 1/4 of the time corresponds to a lake inflow of $1,067$
472 $\text{m}^3 \cdot \text{s}^{-1}$ or $92,204 \text{ m}^3 \cdot \text{d}^{-1}$ with between $0.044\text{-}0.291 \text{ m}^3 \cdot \text{s}^{-1}$ from the feeding tributaries. The lake



473 inflows that are exceeded 5 % of the time correspond to $6.939 \text{ m}^3 \cdot \text{s}^{-1}$ or $599,535 \text{ m}^3 \cdot \text{d}^{-1}$ with
 474 between $0.224\text{-}2.49 \text{ m}^3 \cdot \text{s}^{-1}$ from the feeding tributaries.

Exceedance percentile	Rainfall mm/yr ⁻¹	Verlorenvlei		Kruismans		Bergvallei		Krom Antonies		Hol	
		m ³ ·s ⁻¹	m ³ ·d ⁻¹	m ³ ·s ⁻¹	m ³ ·d ⁻¹	m ³ ·s ⁻¹	m ³ ·d ⁻¹	m ³ ·s ⁻¹	m ³ ·d ⁻¹	m ³ ·s ⁻¹	m ³ ·d ⁻¹
95	227	0.054	4702	0.004	346	0.001	69	0.001	109	0.002	176
90	264	0.074	6356	0.007	604	0.002	191	0.003	232	0.003	269
85	282	0.088	7628	0.010	830	0.004	366	0.004	319	0.004	353
80	290	0.104	8979	0.012	1072	0.007	596	0.005	392	0.005	434
75	296	0.119	10303	0.015	1291	0.010	839	0.005	459	0.006	508
70	324	0.136	11759	0.018	1517	0.013	1104	0.006	534	0.007	587
65	357	0.155	13373	0.021	1791	0.016	1381	0.007	602	0.008	676
60	387	0.176	15180	0.024	2104	0.019	1657	0.008	685	0.009	786
55	396	0.203	17575	0.029	2506	0.023	1965	0.009	772	0.011	913
50	405	0.237	20498	0.035	3032	0.027	2309	0.010	882	0.012	1058
45	422	0.286	24669	0.043	3755	0.032	2807	0.012	1024	0.014	1222
40	430	0.371	32023	0.058	5022	0.041	3511	0.015	1258	0.017	1439
35	437	0.516	44598	0.089	7699	0.053	4613	0.020	1745	0.021	1790
30	444	0.710	61310	0.156	13511	0.076	6599	0.033	2824	0.029	2481
25	454	1.067	92204	0.291	25182	0.123	10619	0.062	5387	0.044	3814
20	481	1.571	135726	0.489	42242	0.223	19295	0.110	9511	0.065	5655
15	498	2.399	207275	0.780	67408	0.421	36354	0.192	16594	0.096	8262
10	537	3.759	324746	1.324	114432	0.885	76477	0.359	31045	0.141	12191
5	575	6.939	599535	2.490	215152	1.884	162795	0.929	80305	0.224	19312

475

476 Table 3: The exceedance probabilities for sub-catchment rainfall and Verlorenvlei, Kruismans,
 477 Bergvallei, Krom Antonies and Hol streamflow in $\text{m}^3 \cdot \text{s}^{-1}$ and $\text{m}^3 \cdot \text{d}^{-1}$

478 6. Discussion

479 6.1 Modelling in sub-Saharan Africa

480 A major limitation facing the development and construction of comprehensive modelling
 481 systems in sub-Saharan Africa is the availability of appropriate climate and streamflow data.
 482 For this study, while there was access to over 20 years of streamflow records, the station was
 483 only able to measure a maximum of $3.675 \text{ m}^3 \cdot \text{s}^{-1}$, which hindered calibration of the model for
 484 high flow events. As such, the confidence in the model's ability to simulate high streamflow
 485 events using climate records is limited. While the availability of measured data is a limitation



486 that could affect the modelled streamflow, discontinuous climate records also hindered the
487 estimations of long time series streamflow.

488 Over the course of the 30-year modelling period, a number of climate stations used for
489 regionalisation were decommissioned and were replaced by stations in different areas. This
490 required climate regionalisation adaption for simulations over the entire 30-year period to
491 incorporate the measured streamflow from the gauging station. To account for missing
492 streamflow records since 2007, an EMD filtering protocol was applied to the runoff data (Fig.
493 6). The results from the EMD filtering showed that after removing the first nine IMFs, the local
494 maxima of both signals match the seasonal water level maxima during most of the years. While
495 considerable improvement can be made to the EMD filtering, the results show some agreement
496 which suggested that the simulated runoff was representative of inflows into the lake.

497 In data scarce catchments it is important to make use of all available data in an effort to improve
498 the understanding of the catchment dynamics. To account for historical gauging data a number
499 of adaptations were made to the climate regionalisation, as well as an EMD filtering protocol to
500 use water level data at the sub-catchment outlet. Consequently, the model performed
501 particularly well considering the streamflow and climate station limitations, although the model
502 is yet to be tested regarding its ability to simulate high flow events.

503 **6.2 Catchment dynamics**

504 Factors that impact on streamflow variability are important for understanding river flow regime
505 dynamics. Previously, factors that affect streamflow variability such as CV and BFI values
506 have been used to determine how susceptible particular river systems are to drought (e.g
507 Hughes and Hannart, 2003). While CV values have been used to account for climatic impacts
508 such as dry and wet cycles, BFI values are associated with runoff generation processes that
509 impact the catchment. For South African river systems, BFI values are generally below 1



510 implying that runoff exceeds baseflow. In comparison CV values can be in excess of 10
511 implying high variability in streamflow volumes (Hughes and Hannart, 2003). Generally, CV
512 and BFI measures have been applied to quaternary river systems in southern Africa. For this
513 study, these two measurements have been used to understand river flow dynamics in much
514 smaller tributaries.

515 The highest proportion of streamflow needed to sustain the Verlorenvlei lake water level is
516 received from the Bergvallei tributary, although the area weighted contribution from the Krom
517 Antonies is more significant (Fig. 7). However, CV values for the Bergvallei indicate high
518 streamflow variability. This is partially due to the high surface runoff component in modelled
519 streamflow within the Bergvallei in comparison to the minor interflow contribution, suggesting
520 little sub-surface runoff. While streamflow from the Bergvallei tributary is 47% groundwater,
521 which would suggest a more sustained streamflow, due to the TMG dominance as well as a
522 high primary aquifer contribution, baseflow from the Bergvallei is driven by highly conductive
523 rock and sediment materials. Similarly, CV values for the Krom Antonies indicate high
524 streamflow variability due to the presence of a high baseflow contribution from the conductive
525 TMG and primary aquifers. Although the Krom Antonies has a larger interflow component,
526 which would reduce streamflow variability, the dominant TMG presence within this tributary
527 partially compensates for the subsurface flow contributions.

528 In contrast, the Hol has a much smaller daily streamflow variability in comparison to both the
529 Bergvallei and the Krom Antonies (Fig. 7). While streamflow from the Hol tributary is mainly
530 comprised of baseflow (56%), the dominance of low conductive shale rock formations as well
531 as a large interflow component result in reduced streamflow variability. While the larger shale
532 dominance in this tributary not only results in a more sustained baseflow from the secondary
533 aquifer, it also results in large interflow due to the limited conductivity of the shale formations.
534 Compounding the more sustained baseflow from the Hol tributary, the reduced presence of the



535 primary aquifer results in a dominance in slow groundwater flow from this tributary. Similarly,
536 the Kruismans is dominated by shale formations which result in a larger interflow contribution,
537 although due to the limited baseflow contribution (14%) the streamflow from this tributary is
538 highly variable, which impacts on its susceptibility to drought.

539 The results from this study have shown that while the Krom Antonies was initially believed to
540 be the major flow contributor, the Bergvallei is in fact the most significant, although
541 streamflow from the four tributaries is highly variable, with baseflow from the Hol tributary
542 the only constant input source. The presence of conductive TMG sandstones and quaternary
543 sediments in both the Krom Antonies and Bergvallei result in quick baseflow responses with
544 little flow attenuation. The potential implication of a constant source of groundwater being
545 provided from the Hol tributary, is that if the groundwater is of poor quality this would result
546 in a constant input of saline groundwater, with the Krom Antonies and Bergvallei providing
547 freshwater after sufficient rainfall.

548 **6.3 Baseflow comparison**

549 The groundwater components of the J2000 model were adjusted using calibrated net recharge
550 and aquifer hydraulic conductivity from a MODFLOW model of one of the main feeding
551 tributaries of the Verlorenvlei. The Krom Antonies was selected for this calibration as it was
552 previously believed to be the largest input of groundwater to Verlorenvlei (Fig. 2). Baseflow
553 for the Krom Antonies tributary was previously calculated using a MODFLOW model (Watson
554 *et al.*, 2018), by considering aquifer hydraulic conductivity and average groundwater recharge.
555 Due to the fact that average recharge was used, baseflow estimates from MODFLOW are likely
556 to fall on the upper end of daily baseflow values. For the Krom Antonies sub-catchment Watson
557 *et al.*, (2018) estimated baseflow between 14,000 to 19,000 m³.d⁻¹ for 2010-2016. In this study,



558 similar daily estimates were only exceeded 10 % of the time, with average estimates (50%) of
559 $1,036 \text{ m}^3 \cdot \text{d}^{-1}$ over course of the modelling period (Fig. 7).

560 Watson et al., (2018) estimates were applied over the course of a wet cycle (2016), and in
561 comparison average baseflow from J2000 for 2016 was $8,214 \text{ m}^3 \cdot \text{d}^{-1}$. The daily timestep nature
562 of the J2000 is likely to result in far lower baseflow estimates, as recharge is only received over
563 a 6-month period as opposed to a yearly average estimate. The possible implication of this is
564 that while common groundwater abstraction scenarios have been based on yearly recharge,
565 abstraction is likely to exceed sustainable volumes during dry months or dry cycles which could
566 hinder the ability of the aquifer to supply baseflow. While the groundwater components of the
567 J2000 have been distributed to allow for improved baseflow estimates, the groundwater
568 calibration was applied to the Krom Antonies. However, this study showed that Bergvallei has
569 been identified as the largest water contributor. In hind sight, the use of geochemistry to
570 identify dominant particular tributaries could have aided the groundwater calibration. While it
571 would have been beneficial to calibrate the groundwater components of the J2000 using the
572 Bergvallei, incorporating one tributary that is dominated by TMG outcrops and one by shale
573 would have improved the representativeness of the baseflow estimates from the model. While
574 the distribution of aquifer components improved modelled baseflow, including groundwater
575 abstraction scenarios in baseflow modelling in the sub-catchment is important for future water
576 management for this ecologically significant area.

577 **6.4 Ecological reserve and evaporative demand**

578 Exceedance probabilities have been used as approximate estimates of minimum river flow
579 requirements. The exceedance percentiles used for ecological reserve determination are
580 streamflow values that are exceeded 95 % of the time (Barker and Kirmond, 1998). For this
581 study, exceedance probabilities were estimated through rainfall/runoff modelling for the



582 previous 30 years within the Verlorenvlei sub-catchment. The exceedance probabilities were
583 determined for each tributary, as well as the total inflows into the lake. These exceedance
584 probabilities were compared with the evaporative demand of the lake, to understand whether
585 inflows are in surplus or whether evaporation demands exceed inflows. As an approximation
586 of the evaporative demand of the Verlorenvlei, an average evaporation loss of 5 mm.d^{-1} was
587 assumed across the lake's surface area (15 km^2).

588 The 95th percentile streamflow contribution, which is the ecological reserve percentile,
589 corresponds to a lake inflow of $4,702 \text{ m}^3.\text{d}^{-1}$, meeting the evaporation demand if the lake was
590 at 7 % capacity. From this it does not seem that the 95th percentile is enough to balance the
591 evaporation demand of the lake. Furthermore, an average streamflow (50th percentile) would
592 only meet the evaporation demand of 1/4 of the lake's surface area. Considering the exceedance
593 probability of the wet cycle period (2007-2017), the 95th percentile corresponded to $7,093$
594 $\text{m}^3.\text{d}^{-1}$, meeting the evaporation demand if the lake was at 10% capacity, while an average
595 inflow (50 percentile) would meet demands if the lake was at 40 % capacity. In contrast, for
596 the dry cycle (1997-2007), the 95 percentile would correspond to a streamflow of $3,438 \text{ m}^3.\text{d}$
597 $^{-1}$, meeting the demand if the lake was at 5 % capacity, while on average (50 percentile) the
598 demands of 15 % of the lake's capacity would be met.

599 From the exceedance probabilities generated in this study, the lake is predominately fed by less
600 frequent large discharge events, where on average the daily inflows to the lake do not sustain
601 the water level above 40 % capacity. This is particularly evident in the measured water level
602 data from station G3T001, where measured water levels have a large daily standard deviation
603 (0.62) (Watson *et al.*, 2018). With climate change likely to impact the length and severity of
604 dry cycles, it is likely that the lake will dry up more frequently into the future, which could
605 have severe implications on the biodiversity that relies on the lake's habitat for survival. Of
606 importance to the lake's survival is the protection of river inflows during wet cycles, where the



607 lake requires these inflows for regeneration and the overallocation of resources could result in
608 prolonged dry cycle conditions.

609 **7. Conclusion**

610 Understanding river flow regime dynamics is important for the management of ecosystems that
611 are sensitive to streamflow fluctuations. While climatic factors impact rainfall volumes during
612 wet and dry cycles, factors that control catchment runoff and baseflow are key to the
613 implementation of river protection strategies. In this study, groundwater components within
614 the J2000 model were distributed to improve baseflow and runoff proportioning for the
615 Verlorenvlei sub-catchment. The J2000 was distributed using groundwater model values for
616 the dominant baseflow tributary, while calibration was applied to the dominant streamflow
617 tributary. The model calibration was hindered by the maximum gauging station resolution,
618 which reduced the confidence in modelling high flow events, although an EMD filtering
619 protocol was applied to account for the resolution limitations and missing streamflow records.
620 The modelling approach would likely be transferable to other partially gauged semi-arid
621 catchments, provided that groundwater recharge is well constrained. The daily timestep nature
622 of the J2000 model allowed for an in-depth understanding of tributary flow regime dynamics,
623 showing that while streamflow variability is influenced by the runoff to baseflow proportion,
624 the host rock or sediment in which groundwater is held is also a factor that must be considered.
625 The modelling results showed that on average the streamflow influxes were not able to meet
626 the evaporation demand of the lake. High-flow events, although they occur infrequently, are
627 responsible for regeneration of the lake's water level and ecology, which illustrates the
628 importance of wet cycles in maintaining biodiversity levels in semi-arid environments. With
629 climate change likely to impact the length and occurrence of dry cycle conditions, wet cycles
630 are important for ecosystem regeneration.



631 **8. Acknowledgements**

632 The authors would like to thank the WRC and SASSCAL for project funding as well as the
633 NRF and Iphakade for bursary support. Agricultural Research Council (ARC) and South
634 African Weather Service (SAWS) for their access to climate and rainfall data.

635 **9. References**

636 Acreman, M. C. and Dunbar, M. J.: Defining environmental river flow requirements – a review,
637 Hydrol. Earth Syst. Sci., 8(5), 861–876, doi:10.5194/hess-8-861-2004, 2004.

638 Barker, I. and Kirmond, A.: Managing surface water abstraction in Wheater, H. and Kirby,
639 C.(eds) Hydrology in a changing environment, voll, Br. Hydrol. Soc. pp249-258, 1998.

640 Batjes, N., Dijkshoorn, K., Van Engelen, V., Fischer, G., Jones, A., Montanarella, L., Petri,
641 M., Prieler, S., Teixeira, E. and Wiberg, D.: Harmonized World Soil Database (version 1.2),
642 Tech. rep., FAO and IIASA, Rome, Italy and Laxenburg, Austria., 2012.

643 Conrad, J., Nel, J. and Wentzel, J.: The challenges and implications of assessing groundwater
644 recharge: A case study-northern Sandveld , Western Cape, South Africa, Water SA, 30(5), 75–
645 81, 2004.

646 Costanza, R., Arge, R., Groot, R. De, Farberk, S., Grasso, M., Hannon, B., Limburg, K.,
647 Naeem, S., O'Neill, R. V, Paruelo, J., Raskin, R. G., Suttonkk, P. and van den Belt, M.: The
648 value of the world ' s ecosystem services and natural capital, Nature, 387(May), 253–260,
649 doi:10.1038/387253a0, 1997.

650 CSIR: Development of the Verlorenvlei estuarine management plan: Situation assessment.
651 Report prepared for the C.A.P.E. Estuaries Programme, , 142 [online] Available from:
652 http://fred.csir.co.za/project/CAPE_Estuaries/documents/Verlorenvlei Situation



- 653 Assesment_Final Draft_Oct2009.pdf, 2009.
- 654 Deb, K., Pratap, A., Agarwal, S. and Meyarivan, T.: A fast and elitist multiobjective genetic
655 algorithm: NSGA-II, IEEE Trans. Evol. Comput., 6(2), 182–197, 2002.
- 656 Domenico, P. A. and Schwartz, F. W.: Physical and Chemical Hydrogeology, John Wiley and
657 Sons, Inc., New York., 1990.
- 658 DWAF: Sandveld Preliminary (Rapid) Reserve Determinations. Langvlei, Jakkals and
659 Verlorenvlei Rivers. Olifants-Doom WMA G30. Surface Volume 1: Final Report Reserve
660 Specifications. DWAF Project Number: 2002-227., 2003.
- 661 Flügel, W.: Delineating hydrological response units by geographical information system
662 analyses for regional hydrological modelling using PRMS/MMS in the drainage basin of the
663 River Bröl, Germany, Hydrol. Process., 9(3-4), 423–436, 1995.
- 664 Harbaugh, Arlen, W.: MODFLOW-2005 , The U . S . Geological Survey Modular Ground-
665 Water Model — the Ground-Water Flow Process, U.S. Geol. Surv. Tech. Methods, 253,
666 doi:U.S. Geological Survey Techniques and Methods 6-A16, 2005.
- 667 Huang, N. E., Shen, Z., Long, S. R., Wu, M. C., Shih, H. H., Zheng, Q., Yen, N.-C., Tung, C.
668 C. and Liu, H. H.: The empirical mode decomposition and the Hilbert spectrum for nonlinear
669 and non-stationary time series analysis, in Proceedings of the Royal Society of London A:
670 mathematical, physical and engineering sciences, vol. 454, pp. 903–995, The Royal Society.,
671 1998.
- 672 Huang, Y., Schmitt, F. G., Lu, Z. and Liu, Y.: Analysis of daily river flow fluctuations using
673 empirical mode decomposition and arbitrary order Hilbert spectral analysis, J. Hydrol., 373(1–
674 2), 103–111, 2009.



- 675 Hughes, D. A.: Providing hydrological information and data analysis tools for the
676 determination of ecological instream flow requirements for South African rivers, *J. Hydrol.*,
677 241(1–2), 140–151, doi:10.1016/S0022-1694(00)00378-4, 2001.
- 678 Hughes, D. A. and Hannart, P.: A desktop model used to provide an initial estimate of the
679 ecological instream flow requirements of rivers in South Africa, *J. Hydrol.*, 270(3–4), 167–
680 181, doi:10.1016/S0022-1694(02)00290-1, 2003.
- 681 Jenson, S. K. and Domingue, J. O.: Extracting topographic structure from digital elevation data
682 for geographic information system analysis, *Photogramm. Eng. Remote Sensing*, 54(11),
683 1593–1600, 1988.
- 684 Kim, N. W., Chung, I. M., Won, Y. S. and Arnold, J. G.: Development and application of the
685 integrated SWAT-MODFLOW model, *J. Hydrol.*, 356(1–2), 1–16,
686 doi:10.1016/j.jhydrol.2008.02.024, 2008.
- 687 King, J. and Louw, D.: Instream flow assessments for regulated rivers in South Africa using
688 the Building Block Methodology, *Aquat. Ecosyst. Health Manag.*, 1(2), 109–124, 1998.
- 689 Kisi, O., Latifoğlu, L. and Latifoğlu, F.: Investigation of empirical mode decomposition in
690 forecasting of hydrological time series, *Water Resour. Manag.*, 28(12), 4045–4057, 2014.
- 691 Krause, P.: Das hydrologische Modellsystem J2000. Beschreibung und Anwendung in großen
692 Flussgebieten, in *Umwelt/Environment*, Vol. 29. Jülich: Research centre., 2001.
- 693 Krause, P., Boyle, D. P. and Bäse, F.: Comparison of different efficiency criteria for
694 hydrological model assessment, *Adv. Geosci.*, 5, 89–97, 2005.
- 695 Lynch, S.: Development of a raster database of annula, monthly and daily rainfall for southern
696 Africa, *Water Res. Comm.*, (1156), 108, doi:10.1024/0301-1526.32.1.54, 2004.



- 697 Martens, K., Davies, B. R., Baxter, A. J. and Meadows, M. E.: A contribution to the taxonomy
698 and ecology of the Ostracoda (Crustacea) from Verlorenvlei (Western Cape, South Africa),
699 African Zool., 31(1), 22–36, 1996.
- 700 Muche, G., Kruger, S., Hillman, T., Josenhans, K., Ribeiro, C., Bazibi, M., Seely, M., Nkonde,
701 E., de Clercq, W. P., Strohbach, B., Kenabatho, K. ., Vogt, R., Kaspar, F., Helmschrot, J. and
702 Jürgens, N.: Climate change and adaptive land management in southern Africa – assessments,
703 changes, challenges, and solutions, in Biodiversity & Ecology, edited by R. Revermann, K. M.
704 Krewenka, U. Schmiedel, J. . Olwoch, J. Helmschrot, and N. Jürgens, pp. 34–43, Klaus Hess
705 Publishers, Göttingen & Windhoek., 2018.
- 706 Pfanschmidt, K.: Optimierungsmethoden zur HRU-basierten N/A-Modellierung für eine
707 operationelle Hochwasservorhersage auf Basis prognostischer Klimadaten des Deutschen
708 Wetterdienstes: Untersuchungen in einem mesoskaligen Einzugsgebiet im Thüringer Wald,
709 2008.
- 710 Pfennig, B., Kipka, H., Wolf, M., Fink, M., Krause, P. and Flügel, W. a.: Development of an
711 extended routing scheme in reference to consideration of multi-dimensional flow relations
712 between hydrological model entities, 18th World IMACS Congr. MODSIM09 Int. Congr.
713 Model. Simulation, Cairns, Aust., (July), 1972–1978 [online] Available from:
714 <http://www.mssanz.org.au/modsim09/F4/pfennig.pdf>, 2009.
- 715 Poff, N. L., Allan, J. D., Bain, M. B., Karr, J. R., Prestegard, K. L., Richter, B. D., Sparks, R.
716 E. and Stromberg, J. C.: A paradigm for river conservation and restoration, Bioscience, 47(11),
717 769–784, doi:10.2307/1313099, 1997.
- 718 Postel, S. and Carpenter, S.: Freshwater ecosystem services, Nature’s Serv. Soc. Depend. Nat.
719 Ecosyst., 195, 1997.



- 720 Postel, S. and Richter, B.: Rivers for life: managing water for people and nature, Island Press.,
721 2012.
- 722 Richter, B. D.: Re-thinking environmental flows: from allocations and reserves to sustainability
723 boundaries, *River Res. Appl.*, 26(8), 1052–1063, 2010.
- 724 Robson, A., Beven, K. and Neal, C.: Towards identifying sources of subsurface flow: A
725 comparison of components identified by a physically based runoff model and those determined
726 by chemical mixing techniques, *Hydrol. Process.*, 6(2), 199–214,
727 doi:10.1002/hyp.3360060208, 1992.
- 728 Rowston, W. S. and Palmer, C. G.: Processes in the development of resource protection
729 provisions on South African Water Law, in *Proceedings of the International Conference on*
730 *Environmental Flows for River Systems*, Cape Town March., 2002.
- 731 Souchon, Y. and Keith, P.: Freshwater fish habitat: science, management, and conservation in
732 France, *Aquat. Ecosyst. Health Manag.*, 4(4), 401–412, 2001.
- 733 SRK: Preliminary Assessment of Impact of the Proposed Riviera Tungsten Mine on
734 Groundwater Resources Preliminary Assessment of Impact of the Proposed Riviera Tungsten
735 Mine on Groundwater Resources, , (392947), 2009.
- 736 Steudel, T., Bagan, R., Kipka, H., Pfennig, B., Fink, M., de Clercq, W., Flügel, W.-A. and
737 Helmschrot, J.: Implementing contour bank farming practices into the J2000 model to improve
738 hydrological and erosion modelling in semi-arid Western Cape Province of South Africa,
739 *Hydrol. Res.*, 46(2), 192, doi:10.2166/nh.2013.164, 2015.
- 740 UMVOTO-SRK: Reconnaissance investigation into the development and utilization of the
741 Table Mountain Group Artesian Groundwater, using the E10 catchment as a pilot study area.,
742 2000.



743 Wagener, T. and Wheater, H. S.: Parameter estimation and regionalization for continuous
744 rainfall-runoff models including uncertainty, *J. Hydrol.*, 320(1–2), 132–154,
745 doi:10.1016/j.jhydrol.2005.07.015, 2006.

746 Watson, A. P., Miller, J. A., Fleischer, M. and de Clercq, W. P.: Estimation of groundwater
747 recharge via percolation outputs from a rainfall/runoff model for the Verlorenvlei estuarine
748 system, west coast, South Africa., *J. Hydrol.*, 558(C), 238–254, doi:10.1016/S1532-
749 0464(03)00032-7, 2018.

750 Wishart, M. J.: The terrestrial invertebrate fauna of a temporary stream in southern Africa,
751 *African Zool.*, 35(2), 193–200, 2000.

752